Universal soliton pattern formations in passively mode-locked fiber lasers

Foued Amrani, Mohamed Salhi, Philippe Grelu, Hervé Leblond, François Sanchez

Universal soliton pattern formations in passively mode-locked fiber lasers

Foued Amrani,[1] Mohamed Salhi,[1] Philippe Grelu,[2] Hervé Leblond,[1] and François Sanchez[1,*]

[1]*Laboratoire de Photonique d'Angers EA 4644, Université d'Angers, 2 Bd Lavoisier, 49000 Angers, France*

[2]*Laboratoire Interdisciplinaire Carnot de Bourgogne, UMR 5209 CNRS—Université de Bourgogne, B.P. 47870, 21078 Dijon, Cedex France*

Corresponding author: francois.sanchez@univ-angers.fr

We investigate multiple-soliton pattern formations in a figure-of-eight passively mode-locked fiber laser. Operation in the anomalous dispersion regime with a double-clad fiber amplifier allows generation of up to several hundreds of solitons per round trip. We report the observation of remarkable soliton distributions: soliton gas, soliton liquid, soliton polycrystal, and soliton crystal, thus indicating the universality of such complexes.   © 2011 Optical Society of America

OCIS codes: 140.3510, 140.7090, 060.5530.

Passively mode-locked fiber lasers have demonstrated their ability to generate several types of soliton complexes, especially in the anomalous dispersion regime where the soliton energy quantization favors multiple pulsing [1]. In particular, bound states of few pulses have been observed independently of both the dispersion regime and the exact physical mechanism of mode locking. For example, bound states have been reported in ring cavities passively mode-locked through nonlinear polarization rotation (NLPR) [2,3] and in figure-of-eight lasers where mode locking is achieved with either a nonlinear amplifying loop mirror (NALM) [4] or a nonlinear optical loop mirror [5]. As mentioned by several authors [6], bound states are an intrinsic feature of fiber lasers and can be considered as a universal dynamical behavior. With this in mind, it is not surprising that historically, bound states have been first predicted with models based on universal equations that do not consider the exact physical mechanism of mode locking, such as the Ginzburg–Landau equation [7–9]. The scaling up of the output power of fiber lasers in recent years has allowed a considerable increase in the number of coexisting solitons in passively mode-locked fiber lasers. Thus, the number of interacting pulses has undergone a big step from a few tens to several hundreds, resulting in new and complex pattern formation dynamics. Concerning such large numbers of self-organized dissipative solitons, all the recent results have been obtained using the nonlinear polarization rotation technique to passively mode lock the fiber laser. A bound state containing several hundreds of pulses was first reported in [10]. By analogy with an atomic lattice, and following the initial suggestion of Mitschke [11], this state was named a soliton crystal. A "rain of solitons" dynamics has also been reported in a similar laser configuration [12]. More recently, several ordered and disordered patterns presenting analogy with the states of matter were observed [13]. A reconstruction has been performed in [14] for a soliton gas, a soliton liquid, a soliton polycrystal, and a soliton crystal. From the theoretical point of view, there are only few predictions concerning the self-organization of a very large assembly of dissipative optical solitons. A model based on a modified cubic Ginzburg–Landau equation had been proposed to describe the soliton crystal formation of infinite extent [15]. An alternative model [1], which reduces to the quintic Ginzburg–Landau equation in the limit of small intensities [16], allowed the description of a soliton crystal of finite extent [17]. The fact that averaged models support soliton crystal solutions suggests that such organized state could be an intrinsic feature of high power fiber lasers independently of the exact mode locking mechanism. This was the initial motivation of the work reported in this paper. We have realized a figure-of-eight fiber laser and demonstrated not only that this configuration can generate a soliton crystal, but also that soliton gas, liquid, and polycrystal states can be observed.

The experimental setup is schematically represented in Fig. 1. It is an all-fiber figure-of-eight laser based on a passive unidirectional ring (UR) cavity that is coupled to a NALM through a 50/50 fiber coupler. The NALM contains a double-clad Er:Yb-doped fiber amplifier manufactured by Keopsys, which consists of a 2.45 m long double-clad fiber (DCF) that has a chromatic dispersion coefficient $\beta_2^{DCF} = -0.0247\,\mathrm{ps^2/m}$ at the operating wavelength $\lambda = 1.55\,\mu\mathrm{m}$, and is pumped at 980 nm by a 4 W semiconductor laser. Two pieces of standard single-mode fiber (SMF 28, $\beta_2^{SMF} = -0.022\,\mathrm{ps^2/m}$) and dispersion-shifted fiber (DSF, $\beta_2^{DSF} = 0.14\,\mathrm{ps^2/m}$) are used to control both the total cavity dispersion and the nonlinearity experienced by mode-locked pulses as
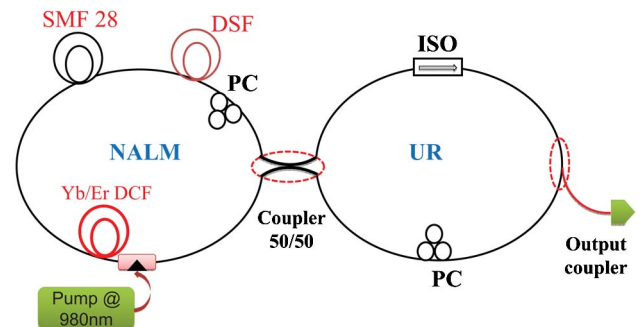

Fig. 1.   (Color online) Experimental setup. DCF, double-clad fiber; DSF, dispersion-shifted fiber; ISO, optical isolator; PC, polarization controller; NALM, nonlinear amplifying loop mirror; UR, unidirectional ring.

they propagate. To favor multiple-pulse mode locking, the total dispersion is set in the anomalous regime with $\beta_2^{TOT}L \approx -0.04\,ps^2$, with a total cavity length of 27.5 m corresponding to a round trip time of 137.6 ns. The UR part is composed of an optical isolator and a 20%-output coupler. For high enough pump power and suitable length of the NALM, mode locking is obtained through the adjustment of the two polarization controllers (PC). The output intensity is detected with a high-speed photodetector (TIA-1200) and visualized with a fast oscilloscope (Tektronix TDS 6124C, 12 GHz, 40 GS/s). The spectral properties are analyzed with an optical spectrum analyzer (Anritsu MS 9710C) and the pulse duration is measured with an optical autocorrelator with a scanning range of ±100 ps (Femtochrome FR-103 XL).

Different soliton patterns can be observed by varying the polarization controllers. The most commonly obtained distribution is a state in which hundreds of solitons fill all the available space along the cavity and are in ceaseless relative motions. The optical spectrum is not modulated and the autocorrelation trace exhibits only a central peak with a very large pedestal. This state can be compared to a "soliton gas", as was reported in NLPR-based fiber lasers [13]. Adjusting the polarization controllers allows switching to a condensed phase that fills about 8% of the cavity, as shown in Fig. 2(a). Although incompletely resolved, real-time recording reveals internal motions of solitons inside the condensed phase that can here be compared to a liquid [13]. Additional insight is obtained from the autocorrelation trace shown in Fig. 2(b) and from the optical spectrum (not shown). The regular spacing of the peaks in the autocorrelation trace indicates an average pulse-to-pulse separation of 11 ps inside packets comprising around 12 solitons. Whereas the total number of solitons is estimated to be as large as 800, these soliton
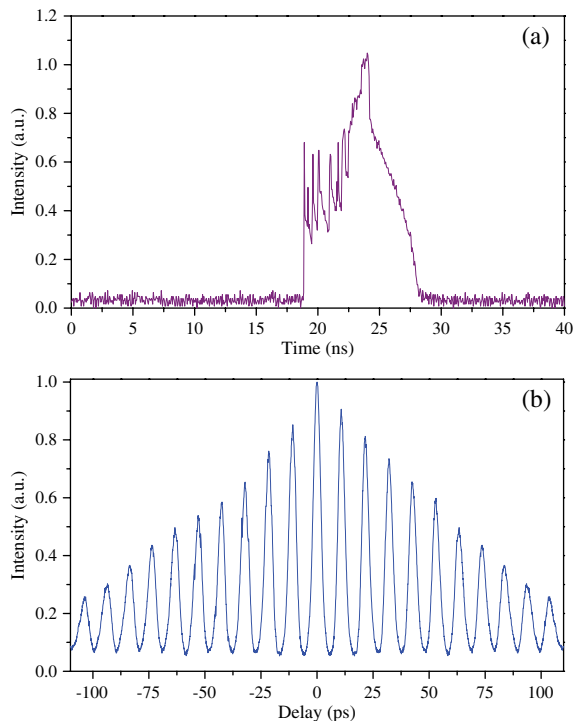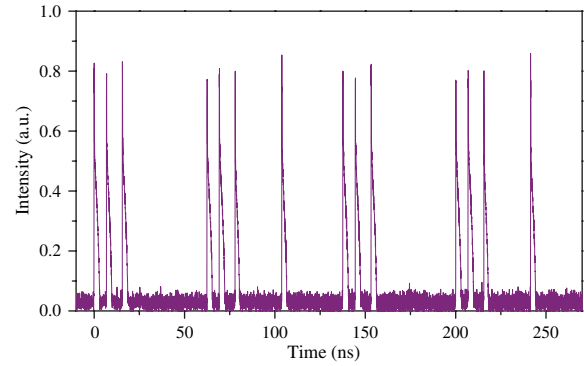

Fig. 3.   (Color online) Temporal trace of a soliton polycrystal.

packets are similar to microdroplets having relative freedom of motion inside the condensed phase. A detailed inspection of Fig. 2(b) indicates that the width of the central peak (4 ps) is significantly smaller than the width of the peaks located at the edge of the scanning range (5.5 ps). This indicates a slightly nonuniform temporal distribution of pulses inside droplets. The pedestal of the autocorrelation trace is also pointing out the lack of a precise separation between all pulses. Finally, the absence of modulation in the spectrum suggests that there is no stable phase relationship between pulses from one round trip to the next.

By slightly varying the polarization controllers we obtained the temporal distribution given in Fig. 3. It consists in a very stable distribution of seven well-separated soliton packets that contain nearly the same amount of solitons. The optical spectrum [Fig. 4(a)] exhibits a strong modulation revealing the high degree of correlation between pulses inside each packet. The spectral period is 2 nm leading to a temporal delay between neighboring

Fig. 2.   (Color online) (a) Temporal trace and (b) autocorrelation trace of a soliton liquid.
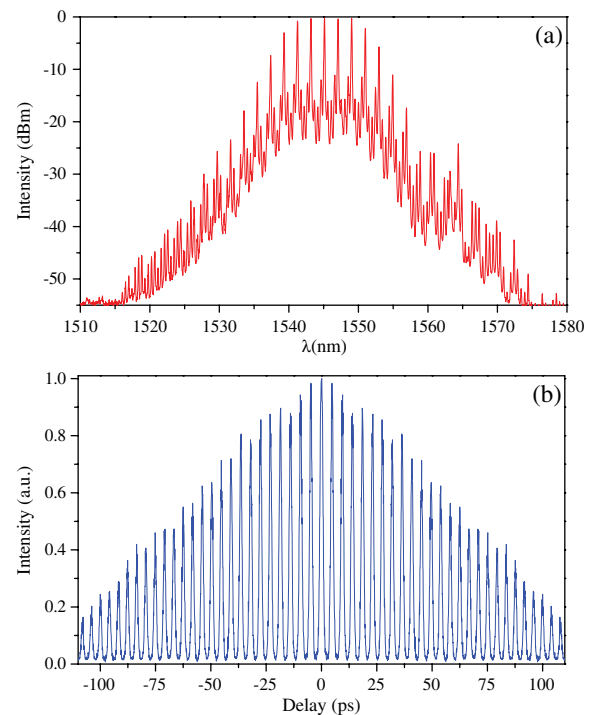

Fig. 4.   (Color online) (a) Optical spectrum and (b) autocorrelation trace of a soliton polycrystal.
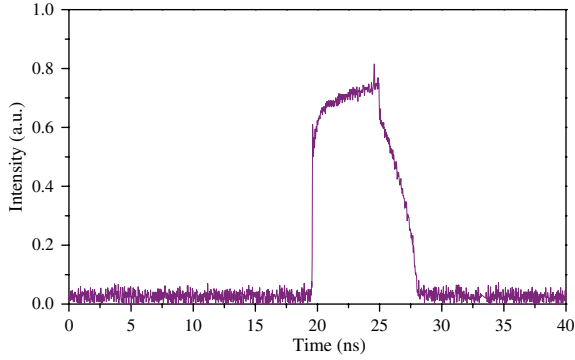
Fig. 5.   (Color online) Temporal trace of a soliton crystal.

pulses of 4.7 ps, as confirmed by the pedestal-free autocorrelation trace of Fig. 4(b). The nearly triangular envelope of the autocorrelation trace, all peaks beneath having the same 1.5 ps width, is characteristic of bound states of regularly spaced solitons [18], and its prolongation till the autocorrelation background indicates a number of roughly 30 bound solitons. The overall soliton distribution inside the cavity is, therefore, an incoherent sequence of small soliton crystals, or crystallites. This soliton pattern is close to the one reported in [13] except that the crystallites are almost identical and well separated inside the cavity.

The last state is remarkable as it consists of a large number of regularly spaced solitons with constant relative phase differences from one round trip to the next. It is a bound state of several hundreds of solitons, or soliton crystal, similar to the cases recently reported in NLPR-based passively mode-locked double-clad fiber lasers [10,15]. The soliton train spans over 7 ns, as indicated by the temporal intensity recording of Fig. 5. The small deviation of the temporal intensity from a rectangular envelope tends to indicate that the soliton packing
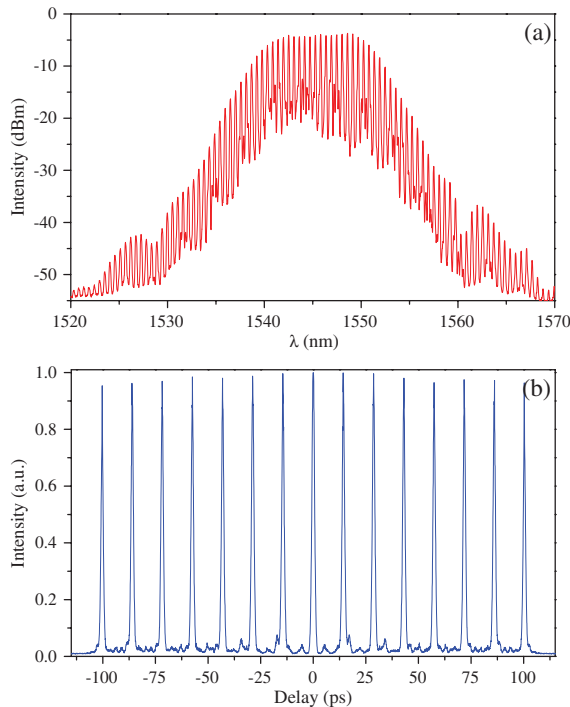
inside the crystal is not perfectly uniform. Note that the trailing edge visible in all time distributions is an artefact due to our detector. However, the corresponding optical spectrum given in Fig. 6(a) proves the strong coherence between pulses since it is modulated with a contrast exceeding 95%. The spectral period is 0.552 nm, which corresponds to a temporal separation of 14.5 ps between solitons, in good agreement with the autocorrelation trace shown in Fig. 6(b), which is mainly composed of 1.5 ps-wide equidistant peaks. From the train duration and the delay between solitons, we estimate the number of pulses in the soliton crystal to be 482.

In summary, we have obtained in the figure-of-eight double-clad fiber laser a variety of soliton patterns and states that were previously observed in double-clad fiber lasers passively mode-locked through nonlinear polarization rotation. More precisely, we have obtained many-soliton states, which, by analogy with the states of matter, can be dubbed as a soliton gas, soliton liquid, soliton crystal, and polycrystal. Our results tend to demonstrate, for the first time, the universality of such soliton states. Indeed, the patterns do not depend on the precise mode locking mechanism. This is a significant step, which provides incentive to developing theoretical approaches based on general dynamical models rather than detailed propagation models meant for a specific subset of mode-locked laser cavities.

Fig. 6.   (Color online) (a) Optical spectrum and (b) autocorrelation trace of a soliton crystal.

References

1. A. Komarov, H. Leblond, and F. Sanchez, Phys. Rev. A **71**, 053809 (2005).
2. D. Y. Tang, W. S. Man, H. Y. Tam, and P. D. Drummond, Phys. Rev. A **64**, 033814 (2001).
3. Ph. Grelu, F. Belhache, F. Gutty, and J. M. Soto-Crespo, Opt. Lett. **27**, 966 (2002).
4. M. J. Guy, D. U. Noske, and J. R. Taylor, Opt. Lett. **18**, 1447 (1993).
5. N. H. Seong and D. Y. Kim, Opt. Lett. **27**, 1321 (2002).
6. J. M. Soto-Crespo and Ph. Grelu, Lect. Notes Phys. **661**, 207 (2005).
7. B. A. Malomed, Phys. Rev. A **44**, 6954 (1991).
8. N. N. Akhmediev, A. Ankiewicz, and J. M. Soto-Crespo, Phys. Rev. Lett. **79**, 4047 (1997).
9. V. V. Afanasjev, B. A. Malomed, and P. L. Chu, Phys. Rev. E **56**, 6020 (1997).
10. A. Haboucha, H. Leblond, M. Salhi, A. Komarov, and F. Sanchez, Opt. Lett. **33**, 524 (2008).
11. B. A. Malomed, A. Schwache, and F. Mitschke, Fib. Int. Opt. **17**, 267 (1998).
12. S. Chouli and Ph. Grelu, Phys. Rev. A **81**, 063829 (2010).
13. F. Amrani, A. Haboucha, M. Salhi, H. Leblond, A. Komarov, and F. Sanchez, Appl. Phys. B **99**, 107 (2010).
14. F. Amrani, M. Salhi, H. Leblond, and F. Sanchez, Opt. Commun. **283**, 5224 (2010).
15. A. Haboucha, H. Leblond, M. Salhi, A. Komarov, and F. Sanchez, Phys. Rev. A **78**, 043806 (2008).
16. A. Komarov, H. Leblond, and F. Sanchez, Phys. Rev. E **72**, 025604(R) (2005).
17. A. Komarov, A. Haboucha, and F. Sanchez, Opt. Lett. **33**, 2254 (2008).
18. F. Gutty, Ph. Grelu, N. Huot, G. Vienne, and G. Millot, Electron. Lett. **37**, 745 (2001).